

Nuclear Track Detectors for Environmental Studies and Radiation Monitoring

S. Manzoor^{a,b,1}, S. Balestra^a, M. Cozzi^a, M. Errico^a, G. Giacomelli^a, M. Giorgini^a, A. Kumar^{a,c},
A. Margiotta^a, E. Medinaceli^a, L. Patrizii^a, V. Popa^{a,d}, I.E. Qureshi^b, and V. Togo^a

^a*Phys. Dept. of the University of Bologna and INFN, Sezione di Bologna, Viale C. Berti Pichat 6/2,
I-40127 Bologna, Italy*

^b*PRD, PINSTECH, P.O. Nilore, Islamabad, Pakistan*

^c*Dept. Of Physics, Sant Longowal Institute of Eng. and Tech., Longowal 148 106 India*

^d*Institute of Space Sciences, Bucharest R-77125, Romania*

Presented at the 10th Topical Seminar on Innovative Particle and Radiation Detectors, 1-5 October 2006, Siena, Italy.

Abstract. Several improvements were made for Nuclear Track Detectors (NTDs) used for environmental studies and for particle searches. A new method was used to determine the bulk etch rate of CR39 and Makrofol NTDs. It is based on the simultaneous measurement of the diameter and of the height of etch-pit cones caused by relativistic heavy ions (158 A GeV Pb⁸²⁺ and In⁴⁹⁺ ions) and their fragments. The use of alcohol in the etching solution improves the surface quality of NTDs and it raises their thresholds. The detectors were used for the determination of nuclear fragmentation cross sections of Iron and Silicon ions of 1.0 and 0.41 GeV/nucleon. These measurements are important for the determination of doses in hadron therapy and for doses received by astronauts. The detectors were also used in the search of massive particles in the cosmic radiation, for the determination of the mass spectrum of cosmic rays and for the evaluation of Po²¹⁰ α -decay and of natural radon concentrations.

1 Introduction

Nuclear Track Detectors (NTDs) were used to search for magnetic monopoles, nuclearites and nuclear fragments with fractional charges [1-3]. They were also been used for the determination of nuclear fragmentation cross-sections [4-6], the measurement of the primary cosmic ray composition [7] and radon measurements [8]. Most studies were performed with CR39 NTDs, which have thresholds of $Z/\beta \geq 5$.

In this paper are described the most favourable etching conditions to obtain the best surface quality and reduce the number of background tracks in the CR39 and Makrofol NTD's used in the Search for Intermediate Mass Magnetic monopoles in SLIM and in other experiments. Formerly we used aqueous solutions of NaOH and KOH [9-11]. The addition of ethyl alcohol in the etchant improves the etched surface quality, reduces the number of surface defects and background tracks at the expense of a higher detection threshold. We studied in detail the etching conditions adding different percentages of ethyl alcohol. Special care was also paid to proper stirring and temperature control of the solutions.

For the study of the response of NTDs we used beams of 158 A GeV Lead and Indium ions at CERN, 1 A GeV Fe²⁶⁺ and Si¹⁴⁺ ions at BNL, USA and 0.41 A GeV Fe²⁶⁺ at HIMAC, Japan.

The NTDs were then used for the determination of fragmentation cross sections and for the detection of environmental contaminations [12].

¹Corresponding author, manzoor@bo.infn.it

2 Experimental

After exposures the detectors were etched in temperature controlled etching baths (to ± 0.1 °C). In order to have a homogeneous solution during the etching and to avoid the deposit of etched products on the detector surfaces, the stirring was kept constant during the whole etching cycle.

The etchants used were water solutions of 6N NaOH and 6N KOH with different fractions of ethyl alcohol. These are called “soft” etching conditions. We also used “strong” etching conditions in order to fastly reduce the thickness of the detectors. For this case we used mainly 8N NaOH, 7N KOH, 8N KOH water solutions. In these conditions many background tracks of 10 to 17 μm range were found; they were probably due to carbon, oxygen and proton recoils produced in the interactions of neutrons. Moreover the surface quality was not very good.

Recently we added alcohol in the following conditions:

Soft etching: For Makrofol we used a 6N KOH solution with 20% ethyl alcohol by volume at 50 °C. For CR39 we used 6N NaOH and KOH at 70 and 60 °C with 1, 2 and 3% ethyl alcohol.

After etching, the detectors were cleaned and dried in air and the etched tracks were measured with the ELBEK automatic measuring system [13].

The presence of alcohol polishes the detector surfaces, improves the transparency of the post-etched detectors and increases the bulk etching velocity.

Strong etching: The Makrofol sheets were etched in 6N KOH solutions with 20% ethyl alcohol at 65 °C for 6 h. The transparency of the detectors was good enough for scanning with a stereo microscope. With this etching condition the thickness was reduced from 500 μm to about 220 μm .

The CR39 sheets from “wagons” exposed at the high altitude Chacaltaya lab. (5230 m a.s.l.) were strongly etched in a solution 8N KOH at 75 °C with 1.5% ethyl alcohol for 30 h.

For soft etching the CR39 threshold is at $Z/\beta \sim 6-7$; for strong etching it is at $Z/\beta \sim 17-19$.

3 Calibration

The bulk-etch rate v_B was previously determined by measuring the mean thickness difference before and after etching; we used an electronic depth-measuring instrument with a 1 μm accuracy.

For relativistic charged particles the track etch rate v_T can be considered constant. We measured v_B by another method; for normally incident particles, the measurable quantities are the cone base diameter D , and the height L_e , see Fig. 1.

The following two relations hold:

$$L_e = (v_T - v_B)t \quad , \quad D = 2v_B t \sqrt{\frac{(v_T - v_B)}{(v_T + v_B)}} \quad (1)$$

From the above two relations the solution for v_B is

$$v_B = \frac{D^2}{4tL_e} \left[1 + \sqrt{1 + \frac{4L_e^2}{D^2}} \right] \quad (2)$$

Relations (1-2) were tested with relativistic Pb and In ions and their fragments in both CR39 and Makrofol NTDs. We selected only those tracks for which precise measurements of the cone height and diameter was possible. Then, using eq. (2) we computed the bulk-etch rate.

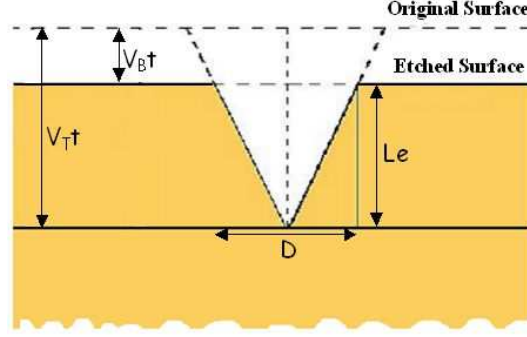


Figure 1: Sketch of an “etched track” in one side of the detector for a normally incident ion.

After “soft” etching of the CR39 and Makrofol sheets the cone base areas of the projectile ions and their fragments were measured with the ELBEK system. Fig. 2a shows the base area distribution of Pb ions and their fragments in Makrofol. The peaks are well separated from $Z/\beta \sim 51$ to 77. The charge resolution close to the Pb peak was improved by measuring the heights of the etch-pit cones (see the inset of Fig. 2b). For each detected nuclear fragment we computed the REL and the reduced etch rate $p=v_T/v_B$ using the formula [14-15]

$$p = \frac{1 + (D/2v_B t)^2}{1 - (D/2v_B t)^2} \quad (3)$$

where 'D' is the diameter of the track, v_T and v_B are the track and bulk etch velocities and t is the etching time.

The reduced etch rate p versus REL is plotted in Figures 3a,b for CR39 and Makrofol. The detection thresholds are at $REL \sim 50$ and $2500 \text{ MeV cm}^2 g^{-1}$ for CR39 and Makrofol detectors, respectively (Fig. 3a). A unique calibration curve was obtained for different high-energy heavy ions in CR39 (Fig. 3b).

4 Total Charge Changing Cross Sections

For the determination of the total charge changing cross sections, σ_{tot} , we used beams of 158 A GeV Pb⁸²⁺ ions, 1 A GeV Fe²⁶⁺ and Si¹⁴⁺ and 0.41 A GeV Fe²⁶⁺ on different targets. We measured the number of incident and survived ions before and after each target material.

The fragmentation charge-changing cross section was evaluated using the formula

$$\sigma_{tot(exp)} = X_T \cdot \ln(N_i / N_s) \quad (4)$$

where $X_T = A_T/\rho_T \cdot t_T \cdot N_A$; N_i is the number of primary ions, N_s the number of survived ions after the target. A_T , ρ_T and t_T are the mass number, density and thickness of the target material.

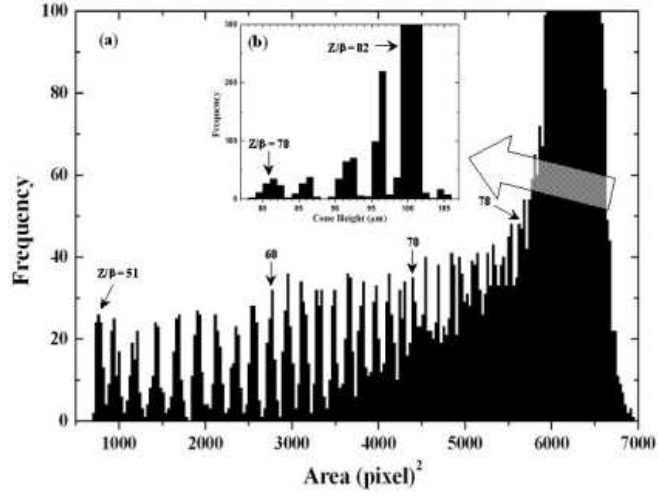


Figure 2: (a) Base area distribution of etched cones in Makrofol from 158 A GeV Pb^{82+} ions and their fragments (averages of 2 front face measurements); (b) cone height distribution for $78 \leq Z/\beta \leq 83$.

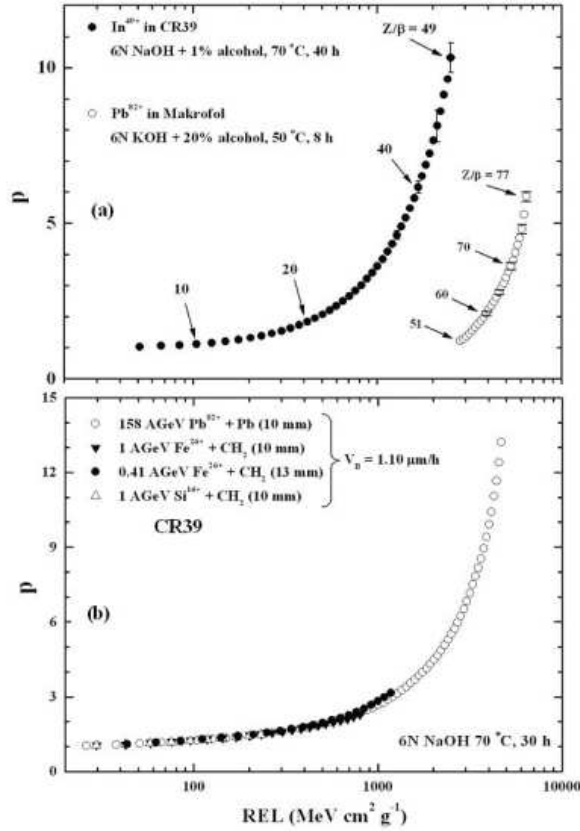


Figure 3: (a) p vs. REL for CR39 and Makrofol NTDs; the points are the data; typical statistical standard deviations are shown; for the other data the errors are inside the data points. (b) p vs. REL for CR39 exposed to energetic Lead, Iron and Silicon ions. The calibrations were made using the new method for v_B .

The cross section on hydrogen was obtained by subtracting the C from the CH₂ total charge changing cross sections using the following relation

$$\sigma_H = \frac{1}{2}(3\sigma_{CH_2} - \sigma_C) \quad (5)$$

These measurements were compared with the calculations based on the equation (see Table 1)

$$\sigma_{tot(theo)} = \pi r_0^2 (A_p^{\frac{1}{3}} + A_t^{\frac{1}{3}} - b)^2 \quad (6)$$

The experimental total charge changing cross sections increase with increasing target mass number. From Table 1 it is seen that for the CH₂ target the total cross sections increase with the increase of the projectile energy.

Target	$t, \rho t$ (g/cm ²)	$\sigma_{tot(exp)}$ (mb)	$\sigma_{tot(theo)}$ (mb)
<i>158 A GeV Pb⁸²⁺</i>			
H	-	1944 ± 275	2120
CH ₂	0.97	2266 ± 156	2616
CR39	4.02	2642 ± 81	2832
C	1.75	2910 ± 210	3113
Al	2.78	3804 ± 164	3742
Cu	8.81	5089 ± 274	4714
<i>Si¹⁴⁺ 1 A GeV</i>			
CH ₂	1.07	1065 ± 140	863
<i>Fe²⁶⁺ 0.41 A GeV</i>			
CH ₂	1.26	1098 ± 110	1249
<i>Fe²⁶⁺ 1 A GeV</i>			
CH ₂	1.07	1206 ± 130	1249
<i>Fe²⁶⁺ 5 A GeV</i>			
CH ₂	0.97	1216 ± 174	1249

Table 1: The measured and computed total charge-changing cross sections for Pb, Fe and Si projectiles on different targets. The data given in the last 4 rows are preliminary. The cross sections on CR39 and CH₂ are averaged on the number of atoms. The quoted uncertainties are statistical only.

5 Alpha Radioactivity Measurement

The α -radioactivity from Po²¹⁰ of the OPERA lead plates with 0.07% Ca or 2.5% Sb were measured with CR39 NTDs and a Surface Barrier Silicon Detector (SBSiD) [16]; comparison of the obtained results are shown in Figure 4. We refreshed the CR39 sheets with our improved etching conditions before α -activity measurements i.e. we removed all the pre exposure α -activity due to radon or defects in CR39 NTDs. The exposure set up is sketched in the inset of Fig. 4.

6 Conclusions

With use of alcohol we have improved the quality of the post etched surface, removed background and enhanced the sharpness of the tracks in CR39 and Makrofol NTDs, but the

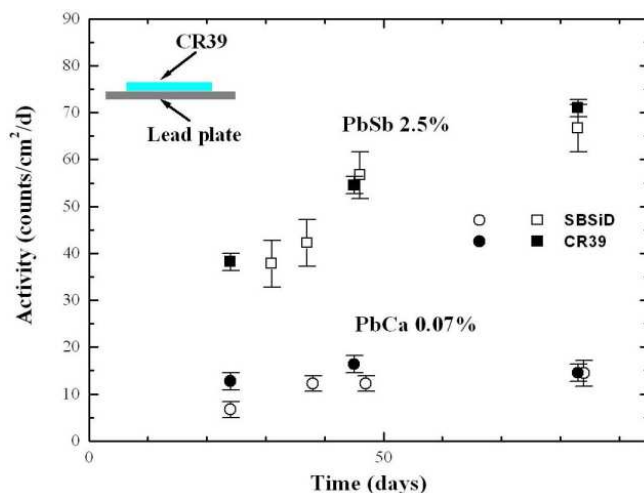


Figure 4: Time dependence of α -radioactivity in PbCa and PbSb plates measured with CR39 NTDs and the SBSiD.

thresholds are higher. New calibration curves were obtained with Pb^{82+} , In^{49+} , Fe^{26+} and Si^{14+} relativistic heavy ions and improved measuring techniques [17-18].

The use of CR39 and Makrofol detectors etched with alcohol can be useful for experiments having a substantial background originated by local sources and in the case of cosmic ray long duration balloon flights, or space experiments.

The measured total charge changing cross sections are in agreement with the calculation based on eq. 6 within statistical standard deviations. On the basis of our results, we conclude that NTDs, especially CR39, can be used for high energy experimental cross section studies.

The improved etching and analysis methods can be applied for the detections of alpha particles from radon and for environmental dosimetry. We successfully applied this new procedure for the measurements of alpha radioactivity in lead plates.

Acknowledgements. We thank the CERN SPS, BNL and HIMAC staff for the beam exposures. We gratefully acknowledge the contribution of our technical staff in Bologna. We thank INFN and ICTP for providing fellowships and grants to non-Italian citizens.

References

- [1] M. Ambrosio et al., Eur. Phys. J. C25 (2002) 511; Nucl. Instrum. Meth. A486 (2002) 663.
- [2] M. Ambrosio et al., Eur. Phys. J. C13 (2000) 453, hep-ex 0009002.
- [3] A. Kumar et al., Radiat. Meas. 36 (2003) 301.
- [4] S. Cecchini et al., Astropart. Phys. 1 (1993) 369.
- [5] S. Cecchini et al., Nucl. Phys. A707 (2002) 513.
- [6] H. Dekhissi et al., Nucl. Phys. A662 (2000) 207.
- [7] T. Chiarusi et al., Radiat. Meas. 36 (2003) 335.

- [8] M. Beozzo et al., Nucl. Tracks Radiat. Meas. 19 (1991) 297.
- [9] S. Cecchini et al., Nuovo Cimento 24C (2001) 639.
- [10] S. Cecchini et al., Nuovo Cimento 109A (1996) 1119.
G. Giacomelli et al., Radiat. Meas. 28 (1997) 217.
- [11] S. Manzoor et al., Nucl. Instrum. Meth. A453 (2000) 525.
- [12] H. A. Khan et al., Radiat. Meas. 31 (1999) 25.
G. Giacomelli et al., hep-ex/0005041.
- [13] A. Noll et al., Nucl. Tracks Radiat. Meas. 15 (1988) 265.
- [14] S. A. Durrani et al., Solid State Nuclear Track Detection, Pergamon press (1987).
- [15] G. Giacomelli et al., Nucl. Instrum. Meth. A411 (1998) 41.
- [16] OPERA Int. Note (2006), Private Comm.
- [17] S. Balestra et al., accepted for publication Nucl. Instrum. Meth. B, physics/0610227.
- [18] V. Togo et al., 10th Inter. Symp. Radiat. Phys., Coimbra, Portugal, 17-22 Sept. 2006:
to be published in Nucl. Instrum. Meth. A, physics/0611105.